PEGylation of Melittin: Structural Characterization and Hemostatic Effects

HENRY T. PENG,* HUANG HUANG AND PANG N. SHEK
Defence Research and Development Canada – Toronto, 1133 Sheppard Avenue West, P.O. Box 2000, Toronto, Ontario, Canada

SOPHIE CHARBONNEAU AND MARK D. BLOSTEIN
Lady Davis Institute of Medical Research, Jewish General Hospital McGill University, Montreal, Quebec, Canada

ABSTRACT: To promote and understand the structure–property relationship for hemostasis, we modified melittin (MLT) using a four-arm poly(ethylene glycol) (PEG) with *N*-hydroxysuccinimide ester. The PEGylation was characterized by FTIR, MALDI-MS, NMR, a bicinchoninic acid assay, circular dichroism, hemolysis assay, and thromboelastography. Changes in the reaction conditions affected the extent of the modification, the numbers of MLT conjugated to PEG arms, and possible PEGylation sites. The reaction at pH 9.2 with a high MLT/PEG ratio, resulted in the highest modification. Reactions in dimethylsulfoxide (DMSO) resulted in more multi-arm coupled MLT, reaching a maximum of four MLT per PEG. The helicity of the modified peptide, relative to the native peptide, was essentially maintained in DMSO, but substantially lost at pH 9.2. PEGylation reduced the hemolytic effects of MLT and subsequently changed its coagulation profiles. The overall hemostatic effects of MLT modified in DMSO indicate that this may be a convenient approach to the PEGylation of biomolecules for biomedical applications.

KEY WORDS: PEGylation, melittin, hemolysis, blood coagulation, bioconjugation.

*Author to whom correspondence should be addressed.
E-mail: henry.peng@drdc-rddc.gc.ca
Figure 2 appears in color online: http://jbc.sagepub.com

0883-9115/10/01 0075–23 $10.00/0 DOI: 10.1177/0883911509354230

INTRODUCTION

Melittin (MLT) has a 26 amino-acid peptide, the sequence; NH_2-GIGAVLKVLTTGLPALISWIKRKRQQ-$CONH_2$, is the main constituent of bee venom, comprising about 50% of its dry weight [1]. An amphipathic molecule with a hydrophobic *N*-terminal region (1–20) and a hydrophilic C-terminus (21–26), MLT has a random coil conformation in dilute aqueous solutions [2]. MLT has two regions of α-helix separated by a proline 'hinge' in aqueous solutions at high concentrations or in hydrophobic environments, such as alcohols or lipid bilayers [3]. The peptide can also self-associate to form a tetramer depending on solvent type and solution condition [4]. The conformation and aggregation of MLT in an aqueous solution depend on several factors including the peptide concentration, ionic strength, pH, and the nature of the ions in a solution [5]. In plasma, MLT appears to be a random coil [6].

MLT has many biological activities including; an antimicrobial agent against Gram-positive and Gram-negative bacteria [7], an anti-inflammatory agent [8], a reagent for gene, and drug delivery [9] as well as for the treatment of arthritic disorders [10] and cancers [11]. Its effects on the cardiovascular system [12] and insulin secretion [13] have also been demonstrated and attributed to the activation of phospholipase A_2. However, MLT is extremely cytotoxic and potentially immunogenic [14] and thus not clinically used. To further understand the structural effects on its biological properties and render it more biocompatible, different methods have been used to modify MLT, including chemical crosslinking [15], acylation [16], and conjugation to polymers [17] and lipids [18]. MLT analogs have been investigated for antibacterial and toxic activities [19], to improve its antimicrobial activity [20] and designs to target specific cells [21]. Most of the studies have been focused on the modification or replacement of MLT residuals with small molecules to understand its structure–function relationship.

Poly(ethylene glycol) (PEG) is widely used to conjugate drugs, proteins, and peptides for potential biomedical applications. The PEG-conjugated compounds are more soluble and have a longer half-life in blood with reduced immunogenicity and toxicity [22,23]. PEG has also been utilized to produce nano-objects and tissue regenerative matrices in combination with helical peptides [24] and biological molecules [25]. Bioconjugation with multiple-arm PEG or 'multi-PEGylation' has been mainly used for making hydrogels [26] and gene delivery [27,28]. New PEGs with multiple functionalities at the end [29] and side groups [30] have been studied as a high drug-loading carrier, overcoming the limited payload of linear PEGs. MLT has only been modified with small

molecules except for polyethylenimine [9] and poly(amidoamine) [17] used for gene delivery.

MLT has been reported to accelerate blood coagulation, presumably through the activation of coagulation factor X, and its binding to the gamma-carboxyglutamic acid domain of factors IXa and X [31]. MLT also acts on blood coagulation through its hemolytic effects on cellular components of blood, particularly on erythrocytes and platelets [32,33]. It was hypothesized that the multi-PEGylation would permit optimum interactions of MLT with blood components for hemostatic effects. The amphipathic helical nature of MLT can be self-assembled to construct supramolecular architectures through a combination with synthetic polymers [34,35]. A self-assembling peptide has promoted complete hemostasis immediately, when applied directly to a wound in the brain, spinal cord, femoral artery, liver, or skin of hamsters [36].

To explore the application of MLT for promoting hemostasis, we modified the peptide with a four-arm PEG *N*-hydroxysuccinimide (NHS) ester under different conditions. The objective of this study is to understand the effects of solution pH, solvent type, and reactant concentrations on the PEGylation and resulting conformation of MLT.

MATERIALS AND METHODS

Materials

MLT, with >90% purity, was purchased from Sigma-Aldrich Canada (Mississauga, ON, Canada). Four-arm PEG-succinimidyl α-methylbutanoate, with a molecular weight of 10,680 Da, was obtained from Nektar Therapeutics (Huntsville, AL, USA). BCA™ Protein Assay Kit was purchased from Fisher Scientific Canada (Nepea, ON, Canada). All other reagents were from various suppliers with the purity of ACS grade or higher.

PEGylation of MLT

PEG (1.2 mg/mL) was dissolved in dimethylsulfoxide (DMSO) and MLT (1.38 mg/mL) was added. The solution was stirred at 150 rpm under room temperature for 18 h and then diluted with 4 × Milli-Q water and dialyzed against Milli-Q water for 3 days, using a dialysis membrane with a molecular weight cut-off (MWCO) of 6–8 kDa (Fisher Scientific Canada, Nepea, ON, Canada). The final product was obtained through freeze-drying of the solution after dialysis.

Prior to the PEGylation in DMSO, MLT was dialyzed with a MWCO of 1200 Da (Sigma-Aldrich Canada, Mississauga, ON, Canada) against

pH 3 HCl for 20 h and lyophilized and designated as DMSO dial. pH 3. The PEGylation was also carried out in dimethylformamide (DMF), and in aqueous buffer solutions with a pH of 9.2, 4.5, and 2.5, respectively, under the same conditions. In addition, the concentrations of MLT and PEG in the reaction were both increased by four-fold while keeping their ratio constant, designated as high concentration (HC). Alternatively, the ratio was increased four-fold by increasing MLT only while keeping PEG concentration unchanged; designated as high MLT/PEG ratio (HR).

Ftir Spectroscopy

Attenuated total reflectance (ATR) Fourier transform infrared spectra of each sample in a powder form were obtained with a Thermo Nicolet IR 100 system using a Zn–Germanium ATR accessory (Thermo Electron Corporation, PA, USA). Each sample was placed against the ATR element and the spectra were collected in the range 800–4000 cm^{-1} using 64 scans at a resolution of 4 cm^{-1}.

Matrix-Assisted Laser Desorption/Ionization Time-of-flight Mass Spectrometer

Mass spectra were acquired in a linear mode at positive polarity on Applied Biosystems Voyager-DE STR matrix-assisted laser desorption/ionization time-of-flight mass spectrometer (MALDI-TOF-MS) equipped with a 337 nm laser. Acceleration voltage was set at 25 kV, grid voltage at 90%, guide wire at 0.02%, delay time at 175 ns, and the mass range was set between 2000 and 30,000 Da. The mass spectra were externally calibrated by the molecular weights of cytochrome C and myoglobin. A saturated sinnapinic acid in 60% acetonitrile/1% acetic acid was used as the matrix solution. Each sample was dissolved in water at a concentration of 10 μg/μL. A 1 μL aliquot of sample solution was mixed with 1 μL of 0.2 μg/μL internal standard (oxidized insulin at *m/z* 3485 Da) in water. Then, 1 μL of this mixture was combined with 1 μL of the matrix solution; 1.5 μL of the obtained solution was spotted on a sample plate. After the crystal was formed, the sample plate was inserted into the mass spectrometer for analysis.

Individual peaks in the spectra were identified for each modified MLT species together with the internal standard; their areas were used to calculate relative PEGylation and percentage for each type of conjugate containing 1–4 MLT molecules [37,38]. The relative PEGylation was defined as the ratio of the total peak area of all PEGylated MLT (PMLT) to that of the internal standard. The percentage of each group of PMLT was calculated as the ratio of the

peak area of the corresponding PEGylated species to the sum of the peak areas generated by all the PMLT.

^{1}H NMR Spectroscopy

^{1}H NMR spectra were obtained on an Ultra500-unity500 spectrometer. D_2O and H_2O at a ratio of 10 : 90 were used as the NMR solvent. Proton resonance assignments of each amino acid in MLT and the ether unit in PEG were based on literature reports [39,40]. The ratio between tryptophan protons (6.9–8.0 ppm) and ethylene oxide protons (3.5–3.8 ppm) was calculated to estimate the number of MLT per PEG molecule [39,41,42]. The weight percentage of PMLT in the conjugate was then calculated based on the ratio and the molecular weights of MLT and PEG.

Bicinchoninic Acid Assay

The bicinchoninic acid (BCA)^{TM} protein assay kit was used to quantify the amount of PMLT in the product. Each product was dissolved in Milli-Q water (0.5 mg/mL). The working reagent was a 50 : 1 ratio BCA reagent A and reagent B. Each PMLT (40 μL) was mixed with 800 μL of the working reagent and incubated at 60°C for 30 min. The reaction solution was then read at 562 nm on a UV-visible spectrophotometer (Agilent Technologies Canada Inc., Mississauga, ON, Canada). PEG and bovine serum albumin solutions in Milli-Q water were used as a negative and positive control, respectively. A standard curve for MLT in Milli-Q water was constructed. The weight percentage of PMLT in the product was calculated as the amount of MLT measured by the BCA assay divided by the total mass of the product.

Circular Dichroism Spectrometry

The circular dichroism (CD) spectra of the original MLT and PMLT in methanol at a 200 μM equivalent peptide concentration were recorded between 200 and 250 nm on a JASCO 810 spectropolarimeter (Jasco Inc., Easton, MD, USA).

Hemolysis

Red blood cells (RBC) were isolated by centrifuging the blood samples from healthy volunteers for 10 min at 6000 rpm and extracting the supernatant. The RBC was washed three times with phosphate buffer saline (PBS) pH 7.4, and suspended in PBS (final 5% v/v). Each solution

was added to a RBC suspension to yield a final volume of 120 μL (2.5% v/v final RBC concentration) and a MLT concentration of 40 μM. The mixture was incubated at 37°C for 1 h and centrifuged for 5 min at 2500 rpm. The supernatant was extracted and diluted with PBS 10-fold. The absorbance was measured under the UV-visible at 540 nm. The same technique was performed using PMLT instead of MLT. For the positive control of 100% hemolysis, 1% v/v Triton X-100 was used to suspend the RBC and for the negative control, RBC suspended in PBS. Both positive and negative controls had a final RBC concentration of 2.5% v/v. The percent hemolysis was calculated using the following equation:

$$\% \text{ Hemolysis} = \left[(A_{\text{sample}} - A_{\text{neg}})/(A_{\text{pos}} - A_{\text{neg}})\right] \times 100\%, \quad (1)$$

where A_{sample}, A_{neg}, and A_{pos} are the absorbance of the sample, negative, and positive controls.

Thromboelastography

For each PMLT sample, the wt% of MLT was predetermined by the BCA assay. Each sample solution was prepared in pH 7.4 Tris buffer to a 720 μM equivalent of MLT. With institutional approval and subject consent, blood samples were taken from healthy volunteers via venipuncture and collected into separate Vacutainers (Fisher Scientific, Nepean, ON) containing 0.109 M sodium citrate solution (citrate : blood volume = 1 : 9) and gently inverted three times. Thromboelastographic (TEG) measurements were carried out using a computerized TEG® Hemostasis System 5000 (Haemoscope Corporation, Niles, IL, USA). Specifically, after the system has passed the electronics testing and quality control according to manufacturer's protocol, a sample solution (20 μL) was pipetted into TEG cups pre-warmed to 37°C. An aliquot of 20 μL of 0.2 M calcium chloride solution and 320 μL of blood were then added into the TEG cups, respectively, giving 40 μM of MLT. The measurement was started immediately and run until all interested parameters were finalized. The Tris buffer of 20 μL was used instead of the sample solution as a negative control. The blood–material interaction was measured by the percent difference for each TEG parameter using the follow equation:

$$\% \text{ Difference from blank} = [(P_s - P_0)/P_0] \times 100\%, \quad (2)$$

where P_s and P_0 are the parameters measured with an agent-dosed sample and a negative control from the same blood draw, respectively.

Statistic Analysis

Data were presented as mean±standard deviation and compared using a two-tailed *t*-test with 95% confidence to identify significantly different groups.

RESULTS

PEGylation of MLT

The modification was confirmed and quantified; shown in Figure 1 are the peptide amide peaks at 1650 and 1540 cm^{-1}, the NHS ester and ether peaks for PEG at 1809, 1781, 1739 (the ester peaks disappeared after the reaction), and 1100 cm^{-1}. Slight shifts in the amide I peak from 1646 to 1650 cm^{-1} was observed but no new peaks were observed as the new amide bonds overlapped with the peptide.

The relative PEGylation and the numbers of arms coupled with MLT were determined by mass spectroscopy. Typical MALDI-TOF MS spectra in Figure 2 indicate the presence of a sharp and strong peak of the insulin standard at *m*/*z* 3482 and a board peak of the PEG control at *m*/*z* 10,368, in agreement with their molecular weights. In contrast,

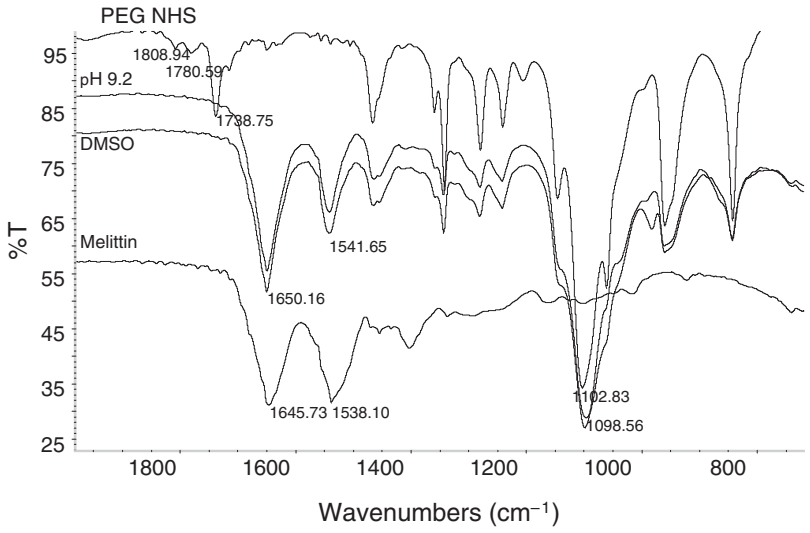

Figure 1. FTIR spectra of PEG NHS ester, MLT and their conjugates prepared in pH 9.2 buffer and DMSO. PEG NHS stands for original four-arm PEG-succinimidyl α-methylbutanoate.

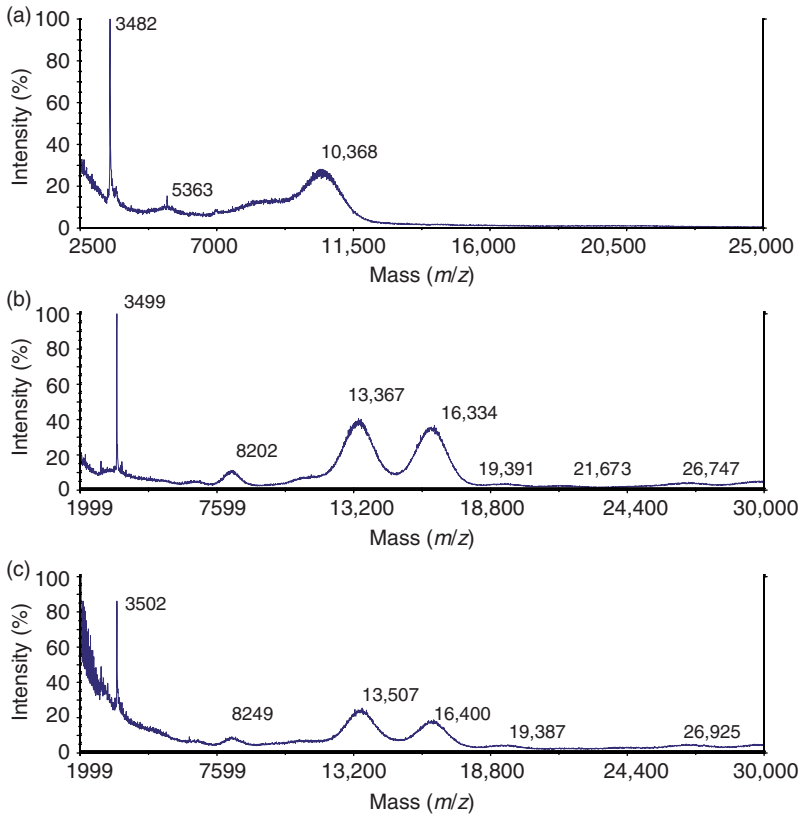

Figure 2. Mass spectra of PEG (a); PEGylated MLT prepared in DMSO (b); and pH 9.2 buffer (c), respectively. Oxidized insulin at m/z 3485 Da was added as an internal standard.

the spectra for the PMLT conjugates corresponded to PEG plus 1–4 MLT molecules with peaks observed at m/z 13,367, 16,334, 19,391, and 21,673 for conjugates with 1, 2, 3, and 4 arms, respectively. The peaks have a normal distribution with widths typical for polydisperse PEG chains. A peak at 26,747, twice the molecular weight of MLT–PEG, implied PEG–MLT–PEG crosslinking. Residuals with molecular weights in the range of 5000–9000 were seen in the spectrum of PEG as well (Figure 2(a)). MLT and hydrolyzed PEG peaks at 2847 and 10,391, for their individual MS spectra, were not noticeable in the spectra of the conjugates (Figure 2(b) and (c)).

The relative PEGylation under different conditions, quantified by total area under the MLT–PEG conjugate peaks and internal standard peak of the MS spectra are shown in Figure 3. Among the

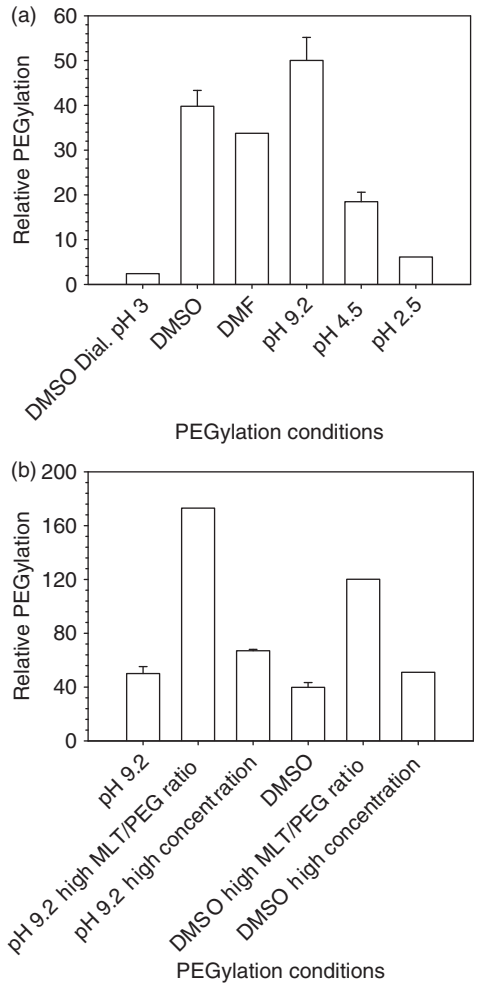

Figure 3. Relative PEGylation under different conditions: (a) Effects of solvent, buffer pH, and (b) MLT to PEG ratio and their concentrations. Error bars are standard deviations ($n = 3$). The relative PEGylation was defined as the ratio of the total peak area of all PMTL to that of the internal standard.

three solvents: aqueous pH 9.2, DMSO, and DMF, the PEGylation appears to be in the same order as their polarities, with pH 9.2 being highest and DMF being lowest (Figure 3(a)). In DMSO, the pre-treatment of MLT, through membrane dialysis against pH 3 HCl, resulted in different PEGylation from the untreated one. In aqueous buffer solutions, the overall extent of modification decreased with solution pH. The effects of MLT to PEG ratio and their concentrations

in pH 9.2 aqueous buffer and DMSO on the production of PEG–MLT adducts are shown in Figure 3(b). In both solvents, the degree of MLT modification by the four-arm PEG increased with MLT: PEG ratio, but to a lesser extent with their concentrations.

The relative abundance of each type of PMLT is shown in Figure 4. The PEGylation in DMSO, using MLT dialyzed against pH 3 was 95%

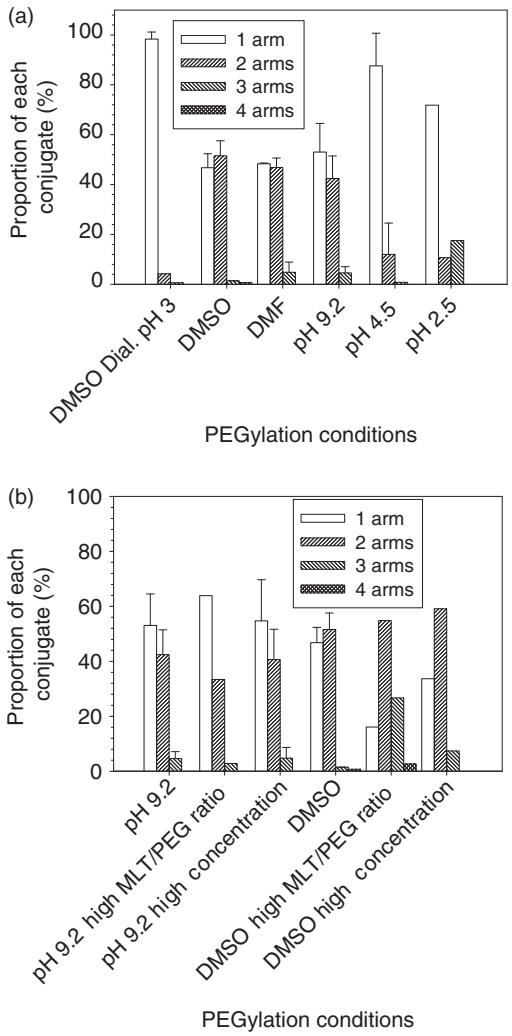

Figure 4. Effects of PEGylation conditions on the distribution of the conjugates containing different numbers of MLT linked to each PEG chain (SD, $n = 3$).

single-arm product, with less at pH 4.5 and 2.5 (Figure 4(a)). The reaction in DMSO also yielded more two arms of PEG–MLT conjugates than buffers and DMF. All 4-arm PEG–MLT only occurred in DMSO. The distribution of each product was not markedly affected by the reactants ratio or concentration in pH 9.2 (Figure 4(b)). In contrast, the multiple-arm conjugates were increased under these conditions in DMSO.

The conjugation was confirmed by NMR spectra of the ethylene oxide resonance for PEG at 3.7 ppm [41] and the aromatic tryptophan residue of MLT at 6.9–8 ppm [43]. The quantitative analysis (Table 1) indicates that an average of 0.4–1.5 out of four arms of PEG had been functionalized with MLT. PEGylation in DMSO at the high ratio led to the highest MLT loading, in contrast with the lowest loading, under the condition designated as DMSO dial. pH 3. An absolute quantification of PEGylation, using a simple BCA assay, is summarized in Figure 5, which shows similar trend effects by PEGylation as seen in the MS and NMR spectra. The BCA test indicates less difference in PEGylation between pH 9.2 and DMSO than seen in the MS spectrum.

Structural Analysis of MLT Before and After Modification

Based on the CD spectra, the MLT and its PEG conjugates prepared under different conditions have different secondary structures (Figure 6). The two minima at 222 and 210 nm are typical of α-helical conformations while the single minimum at 210 nm indicates random structures [5]. The ellipticity values at 222 nm ranging from −15,924 to −591,114 deg cm^2/mol were used to calculate the helicities of MLT before and after the conjugation [16]. It seems that the helix content decreased in the following order of solvents used for PEGylation: DMSO > DMF > pH 4.5 > pH 9.2 phosphate buffer. The ratio and concentration of MLT and PEG had minimal effects.

Table 1. ^{1}H NMR quantification of MLT PEGylation.

PEGylation conditions	Tryptophan/ CH_2CH_2O	PEGylated MLT wt%
pH 9.2	0.88	19.7
pH 9.2 HC[a]	0.95	21.2
DMSO	0.76	17.5
DMSO HR[a]	1.45	28.8
DMSO pH 3	0.40	10.1

Note: [a]HC and HR stand for high MLT and PEG concentration and ratio, respectively.

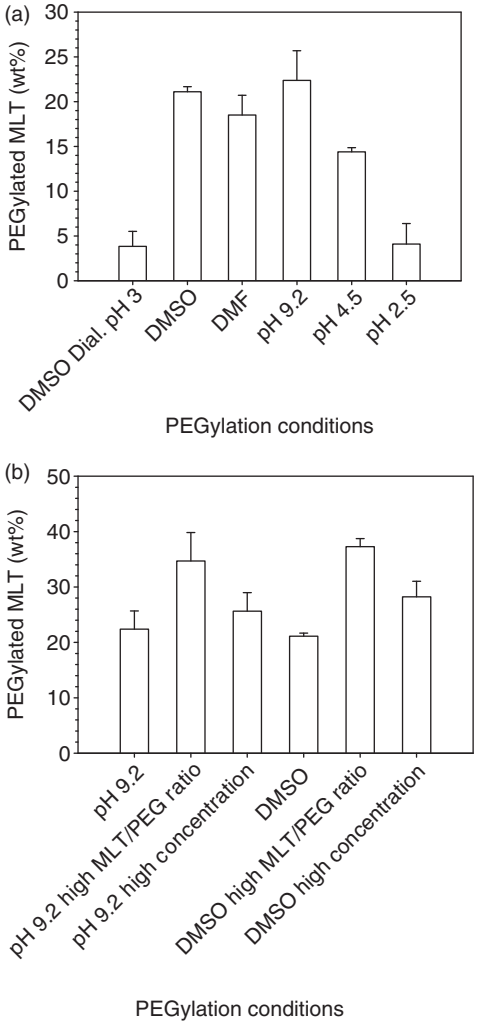

Figure 5. BCA quantification of MLT PEGylation under different concentrations (SD, $n = 3$).

Hemolysis

MLT released $99.5 \pm 1.4\%$ of the hemoglobin at $40\,\mu M$ relative to Triton X-100 (Figure 7). The MLT conjugates led to approximate 10–80% hemolysis depending on preparation conditions, with 10% in pH 9.2 and 80% by the DMSO-PEGylated. In contrast, PEG exhibited minimal hemolysis. The extent in hemolysis can be ranked in the same order as that of helicity retained after PEGylation (Figure 6).

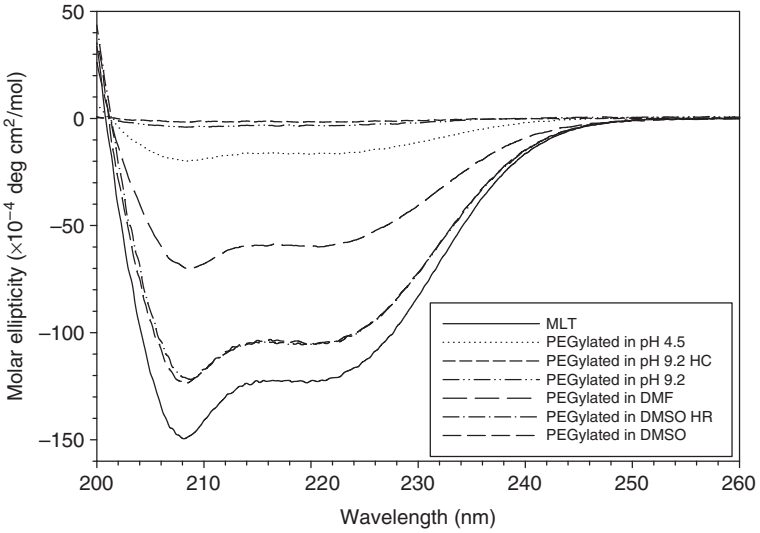

Figure 6. CD spectra of MLT before and after PEGylation.

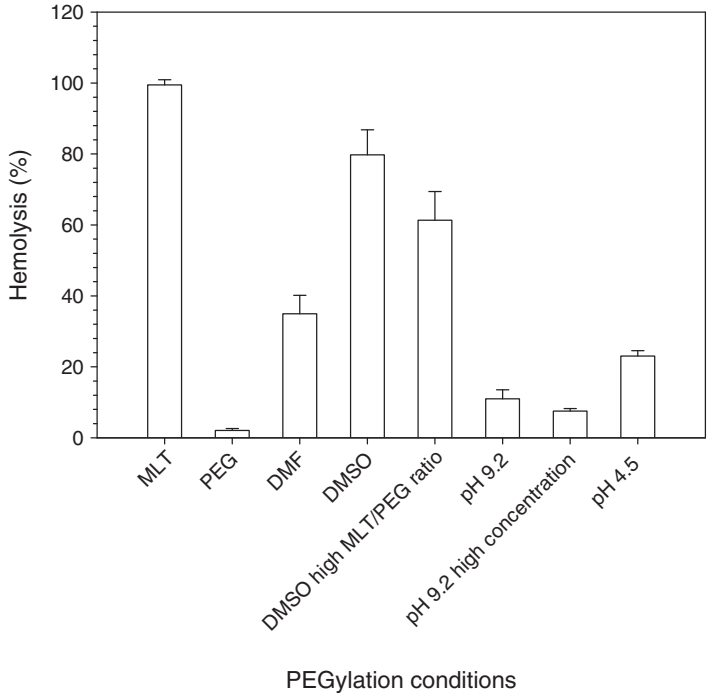

Figure 7. Hemolysis of MLT, PEG, and their conjugates on RBCs (SD, $n = 3$).

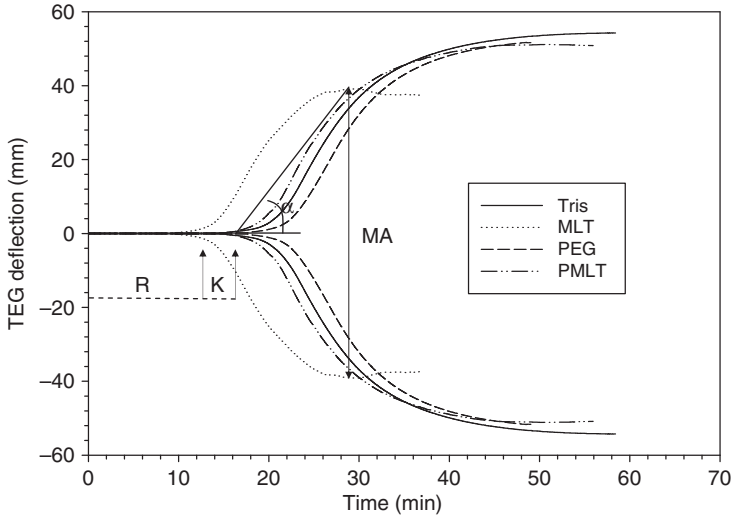

Figure 8. Typical TEG tracings of MLT PEGylated in DMSO (PMLT), compared to the controls (i.e., Tris buffer, MLT, and PEG, respectively). R is the time from the beginning of measurement to the onset of clot formation when the amplitude reaches 2 mm in the TEG tracing; K is taken from the measurement of R to the point at which the amplitude reaches 20 mm; α angle is between the line in the middle of the TEG and the line tangential to the tracing, representing the rate of clot formation; MA is the maximum amplitude, depicting maximum clot strength.

Thromboelastography

TEG measures the *in situ* change in viscosity of blood as a function of time under a low shear and globally measures blood clotting [44]. The measurement is graphically represented as a characteristic shape profile over time (Figure 8), from which, different parameters can be derived. The thromboelastographs for citrated whole human blood with blank (Tris buffer), free MLT, PEG, and PMLT solutions (Figure 8) elucidate four key TEG parameters: (1) time to detectable clot formation (R) (the amplitude = 2 mm in the TEG tracing); (2) time from the measurement of R to the point where the tracing amplitude reaches 20 mm (K); (3) the slope of the tangent joining the point of initial split intercepting the tracing, representing the rate of clot formation (α); and (4) maximum amplitude depicting clot strength (MA). The earliest onset of clot formation (R time) and the weakest clot (maximal amplitude MA, Figure 8) were by MLT; PEGylation shortened R time compared to the controls (PEG in Tris buffer and Tris buffer).

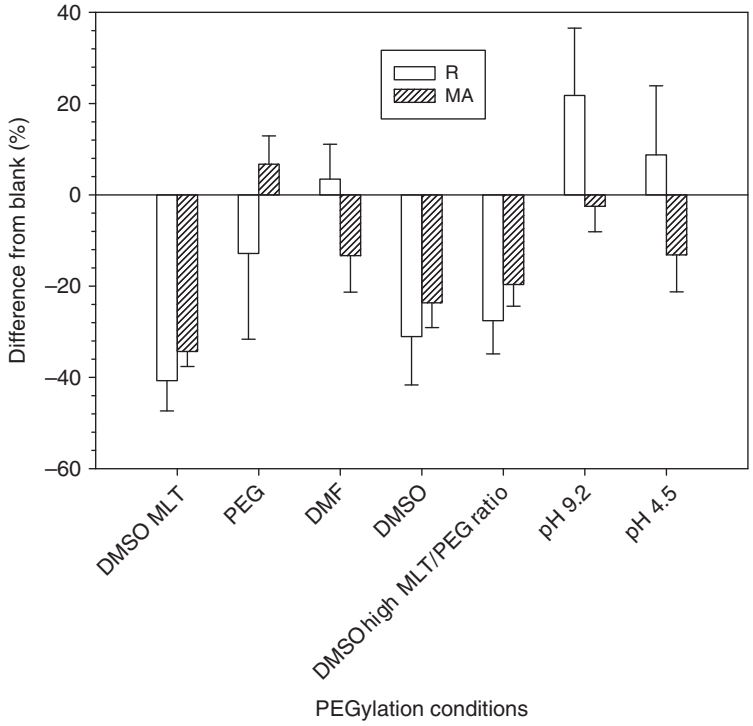

Figure 9. Effects of PEGylation on clotting time (R) and clot strength (MA) (SD, $n = 3$). The final conjugate concentration was 40 μM expressed as bound MLT.

To account for the differences in the blood drawn from different donors and/or at different times, the percent difference of the onset of clot formation and maximal clot strength between the sample and the blank from the same blood was calculated, respectively, and summarized in Figure 9.

The negative changes in R and positive changes in MA indicate an enhancement of clot formation and strength. The magnitude suggests the extent of the effects. In general, PEGylation led to negative effects on the clotting time and positive effects on the clot strength, to different extents depending on its conditions. PEGylation in DMSO led to a reduction in the clotting time comparable to MLT, but less deterioration of the clot strength, improving the overall hemostatic effects. The PEG control had no profound effects on blood coagulation. The hemolysis and initial coagulation times and maximum clot strengths are shown in Figure 10; both R and MA values decrease with increasing hemolysis.

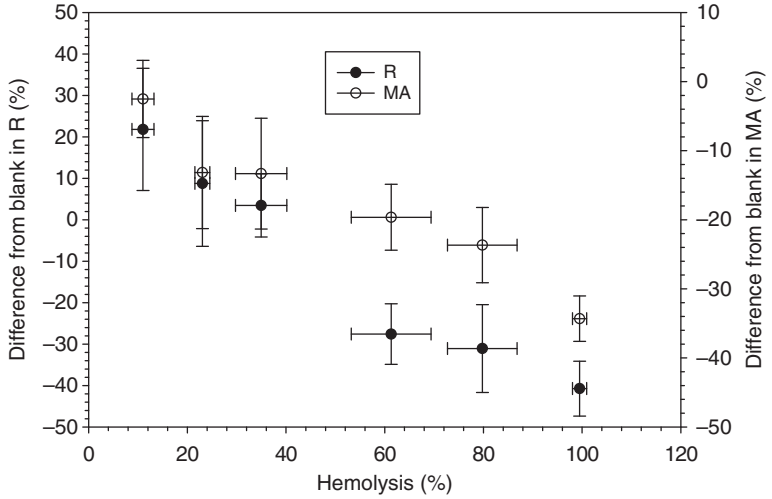

Figure 10. Correlation between hemolysis and blood coagulation (SD, $n = 3$).

DISCUSSION

There are only a few studies that used multiple-arm PEG to modify peptides [41] and drugs [45], to prepare hydrogels [46,47] and improve drug solubility [45]. There are fewer studies that optimized the PEGylation of peptides for biological studies and characterized the impact of individual modifications through each arm [48]. Our study used a multi-arm PEG to increase the drug payload; thus allowing for the optimization of MLT interactions with biological systems [27].

A molecule larger than four MLTs per PEG may be associated with multiple PEGs conjugated to MLT despite the possible steric hindrance (bulky structure) of PEG. There were no noticeable species with molecular weights higher than 30,000 or 40,000. It is noteworthy that the MS used could characterize bioconjugates with a molecular weights higher than 60,000 [49].

An increase in PEGylation at higher pH is due to more amine groups being deprotonated, which is in accordance with the literature on the pH dependence of PEGylation [50–53]. Since the *N*-terminal glycine amine generally has a lower pK_a (~7–8) than the ε-amine of the three side lysines (9–10), at acidic pH 2.5 and 4.5, PEGylation at the *N*-terminal should dominate, resulting in better selectivity for the modification site but a lower degree of the modification. This is

consistent with limited PEGylation in DMSO of MLT pre-dialyzed against pH 3 HCl where peptide amino groups were mostly protonated. Our results are also in agreement with the reports on the site-specific PEGylation at the *N*-terminus by lowing reaction pH [54,55], on the predominant *N*-terminal modification by poly(amidoamine) [17] and acetylation of MLT in a solution with pH below the pK_a value of the *N*-terminal amino group [56]. At pH 9.2, it is likely that PEGylation at the ε-amino group on lysine prevailed since it is more reactive than the α-amino group at the *N*-terminus, when both were not protonated [57].

Self-association occurred in pH 9.2 at MLT concentrations above 3 mM was accompanied by an increased α-helix content above 70% [5,58]. The PEGylation was conducted at the same MLT/PEG molar ratio, but at different MLT concentrations (0.49 and 2.62 mM) in pH 9.2, where MLT may possess dominantly a random coil and helical conformations without aggregation, respectively, and have different accessibilities and mobilities of amines for PEGylation [59]. The effects of PEGylation on the helicity of MLT (Figure 6) may be ascribed to the PEGylation sites involved and are in agreement with literature describing site-dependent PEGylation effects on the secondary structures of helical peptides [60].

Both the PEGylation site and the number of MLT per PEG were taken into account in determining the effects of modification on blood interactions. An amphipathic α-helical structure is essential for the hemolytic activity of MLT [4] and the importance for hemolytic activities of the four amino acids containing primary amino groups appear to follow the following order: lysine 7, *N*-terminal glycine, lysine 21 and lysine 23 [61–63]. The greater decrease in hemolytic activity by MLT modified at a lower pH, where PEGylation was mostly at the *N*-terminal, is similar to that was observed by acetylation of the *N*-terminal residue of MLT [62]. The lower reduction in hemolysis by the PEG conjugation made at a higher pH, where lysine modification was dominant, is consistent with the effects reported for lysine residues on MLT conformations and bioactivities [16,53].

The anticoagulant effects of MLT on whole blood have been ascribed to its inactivation of phospholipids [64]. Our study showed a reduction in coagulation time and clot strength, as indicated by the shorter R and smaller MA, respectively. The hemolysates from erythrocytes and platelets reduce coagulation time, while the destruction of platelets causes a decrease in clot strength [33]. In addition, MLT may activate coagulation factors [31], leading to the decreased R time and faster clotting.

CONCLUSIONS

The overall extent of MLT PEGylation, the number of the peptides per PEG and the conformation of PMLT varied depending on the reaction conditions. MLT PEGylation reduced peptide hemolytic effects, based on hemolysis assay and TEG. The reduced hemolysis may be related to the remaining helicity of the PMLT, which led to a reduction in the coagulation time and maximum clot strength. Thus, the overall hemostatic effects of MLT can be optimized by the PEGylation. Other studies on the potential bioactivity of PMLT with respect to antibacterial and drug delivery effects may be usefully explored for other biomedical applications.

ACKNOWLEDGMENT

The authors are grateful to Tao Xue, Clark Chen, Doug Saunders, and Heather Wright for their excellent technical assistance.

REFERENCES

1. Gauldie, J., Hanson, J.M., Rumjanek, F.D., Shipolini, R.A. and Vernon, C.A. (1976). The Peptide Components of Bee Venom, *Eur. J. Biochem.*, **61**: 369–376.
2. Terwilliger, T.C. and Eisenberg, D. (1982). The Structure of Melittin II. Interpretation of the Structure, *J. Biol. Chem.*, **257**: 6016–6022.
3. Bazzo, R., Tappin, M.J., Pastore, A., Harvey, T.S., Carver, J.A. and Campbell, I.D. (1998). The Structure of Melittin A 1H-NMR Study in Methanol, *Eur. J. Biochem.*, **173**: 139–146.
4. Weaver, A.J., Kemple, M.D. and Prendergast, F.G. (1989). Characterization of Selectively 13C-labeled Synthetic Melittin and Melittin Analogues in Isotropic Solvents by Circular Dichroism, Fluorescence, and NMR Spectroscopy, *Biochemistry*, **28**: 8614–8623.
5. Bello, J., Bello, H.R. and Grandados, E. (1982). Conformation and Aggregation of Melittin: Dependence on pH and Concentration, *Biochemistry*, **2**: 461–465.
6. Terra, R.M.S., Guimarães, J.A. and Verli, H. (2007). Structural and Functional Behavior of Biologically Active Monomeric Melittin, *J. Mol. Graph. Model*, **25**: 767–772.
7. Asthana, N., Yadav, S.P. and Ghosh, J.K. (2004). Dissection of Antibacterial and Toxic Activity of Melittin, *J. Biol. Chem.*, **279**: 55042–55050.

8. Park, H.J., Son, D.J., Lee, C.W., Choi, M.S., Lee, U.S., Song, H.S. et al. (2007). Melittin Inhibits Inflammatory Target Gene Expression and Mediator Generation via Interaction with Iκb Kinase, *Biochem. Pharmacol.*, **73**: 237–247.
9. Boeckle, S., Fahrmeir, J., Roedl, W., Ogris, M. and Wagner, E. (2006). Melittin Analogs with High Lytic Activity at Endosomal pH Enhance Transfection with Purified Targeted PEI Polyplexes, *J. Control. Rel.*, **112**: 240–248.
10. Cui, F., Cun, D., Tao, A., Yang, M., Shi, K., Zhao, M. et al. (2005). Preparation and Characterization of Melittin-loaded Poly(DL-lactic acid) or Poly(DL-lactic-co-glycolic acid) Microspheres Made by the Double Emulsion Method, *J. Control. Rel.*, **107**: 310–319.
11. Holle, L., Song, W., Holle, E., Wei, Y.-Z., Wagner, T. and Yu, X.-Z. (2003). A Matrix Metalloproteinase 2 Cleavable Melittin/Advidin Conjugate Specifically Targets Tumor Cells *In Vitro* and *In Vivo*, *Int. J. Oncol.*, **22**: 93–98.
12. Yalcin, M., Ak, F. and Erturk, M. (2006). The Role of the Central Thromboxane A_2 in Cardiovascular Effects of a Phospholipase A_2 Activator Melittin Administrated Intracerebroventricularly in Normotensive Conscious Rats, *Neuropeptides*, **40**: 207–212.
13. Morgan, N.G., Rumford, G.M. and Montague, W. (1985). Studies on the Mechanism by which Melittin Stimulates Insulin Secretion from Isolated Rate Islets of Langerhans, *Biochim. Biophys. Acta*, **845**: 525–532.
14. Zhao, Z., Rolli, H. and Schneider, C.H. (1995). Immunogenicity of Dinitrocarboxyphenylated Melittin: The Influence of C-Terminal Chain Shortening, N-Terminal Substitution and Prolin Insertion at Positions 5 and 10, *J. Pept. Sci.*, **1**: 140–148.
15. Hider, R.C., Khader, F. and Tatham, A.S. (1983). Lytic Activity of Monomeric and Oligomeric Melittin, *Biochim. Biophys. Acta*, **728**: 206–214.
16. Ramalingam, K., Aimoto, S. and Bello, J. (1992). Conformational Studies of Anionic Melittin Analogues: Effect of Peptide Concentration, pH, Ionic Strength, and Temperature-Models for Protein Folding and Halophilic Proteins, *Biopolymers*, **32**: 981–992.
17. Lavignac, N., Lazenby, M., Franchini, J., Ferruti, P. and Duncan, R. (2005). Synthesis and Preliminary Evaluation of Poly(Amidoamine)–Melittin Conjugates as Endosomolytic Polymers and/or Potential Anticancer Therapeutics, *Int. J. Pharm.*, **300**: 102–112.
18. Legendre, J.Y., Trzeciak, A., Bohrmann, B., Deuschle, U., Kitas, E. and Supersaxo, A. (1997). Dioleoylmelittin as a Novel Serum-Insensitive Reagent for Efficient Transfection of Mammalian Cells, *Bioconjug. Chem.*, **8**: 57–63.
19. Asthana, N., Yadav, S.P. and Ghosh, J.K. (2004). Dissection of Antibacterial and Toxic Activity of Melittin, *J. Biol. Chem.,* **279**: 55042–55050.

20. Sun, X., Chen, S., Li, S., Yan, H., Fan, Y. and Mi, H. (2005). Deletion of Two C-Terminal Gln Residues of 12-26-Residue Fragment of Melittin Improves its Antimicrobial Activity, *Peptides*, **26**: 369–375.
21. Ahmad, A., Yadav, S.P., Asthana, N., Mitra, K., Srivastava, S.P. and Ghosh, J.K. (2006). Utilization of an Amphipathic Leucine Zipper Sequence to Design Antibacterial Peptides with Simultaneous Modulation of Toxic Activity against Human Red Blood Cells, *J. Biol. Chem.*, **281**: 22029–22038.
22. Harris, J.M. and Chess, R.B. (2003). Effect of Pegylation on Pharmaceuticals, *Nat. Rev. Drug Discov.*, **2**: 214–221.
23. Veronese, F.M. and Pasut, G. (2005). PEGylation, Successful Approach to Drug Delivery, *Drug Discov. Today*, **10**: 1451–1458.
24. Vandermeulen, G.W.M., Hinderberger, D., Xu, H., Sheiko, S.S., Jeschke, G. and Klok, H.-A. (2004). Structure and Dynamics of Self-Assembled Poly(Ethylene Glycol) Based Coiled-Coil Nano-Objects, *ChemPhysChem.*, **5**: 488–494.
25. Lih, E, Joung, Y.K., Bae, J.W. and Park, K.D. (2008). An *In Situ* Gel-Forming Heparin-Conjugated PLGA–PEG–PLGA Copolymer, *J. Bioact. Compat. Polym.*, **23**: 444–457.
26. Sanborn, T.J., Messersmith, P.B. and Barron, A.E. (2002). *In Situ* Crosslinking of a Biomimetic Peptide-PEG Hydrogel via Thermally Triggered Activation of Factor XIII, *Biomaterials*, **23**: 2703–2710.
27. Fichter, K.M., Zhang, L., Kiick, K.L. and Reineke, T.M. (2008). Peptide-Functionalized Poly(Ethylene Glycol) Star Polymers: DNA Delivery Vehicles with Multivalent Molecular Architecture, *Bioconjug. Chem.*, **19**: 76–88.
28. Schmieder, A.H., Grabski, L.E., Moore, N.M., Dempsey, L.A. and Sakiyama-Elbert, S.E. (2007). Development of Novel Poly(Ethylene Glycol)-based Vehicles for Gene Delivery, *Biotechnol. Bioeng.*, **96**: 967–976.
29. Schiavon, O., Pasut, G., Moro, S., Orsolini, P., Guiotto, A. and Veronese, F.M. (2004). PEG–Ara-C Conjugates for Controlled Release, *Eur. J. Med. Chem.*, **39**: 123–133.
30. Mero, A., Schivavon, O., Pasut, G., Veronese, F.M., Emilitri, E. and Ferruti, P. (2009). A Biodegradable Polymeric Carrier Based on PEG for Drug Delivery, *J. Bioact. Compat. Polym.*, **24**: 220–234.
31. Blostein, M.D., Rigby, A.C., Furie, B., Furie, B.C. and Gilbert, G.G. (2000). Amphipathic Helices Support Function of Blood Coagulation Factor IXa, *Biochemistry*, **39**: 12000–12006.
32. Stief, T.W. (2007). Thrombin Generation by Hemolysis, *Blood Coagul. Fibrinolysis*, **18**: 61–66.
33. Triantaphyllopoulos, E. (1970). Hemolysis and Blood Coagulation: Evidence of Inhibitory Effects, *Life Sci.*, **7, part II**: 99–110.
34. Woolfson, D.N. and Ryadnov, M.G. (2006). Peptide-Based Fibrous Biomaterials: Some Things Old, New and Borrowed, *Curr. Opin. Chem. Biol.*, **10**: 559–567.

35. Klok, H.-A. (2005). Biological-Synthetic Hybrid Block Copolymers: Combining the Best from Two Worlds, *J. Polym. Sci.*, **43**: 1–17.
36. Ellis-Behnke, R.G., Liang, Y.-X., Tay, D.K.C., Kau, P.W.F., Schneider, G.E., Zhang, S. et al. (2006). Nano Hemostat Solution: Immediate Hemostasis at the Nanoscale, *Nanomed: Nanotech. Biol. Med.*, **2**: 207–215.
37. Chowdhury, S.P., Doleman, M. and Johnston, D. (1995). Fingerprinting Proteins Coupled with Polymers by Mass Spectrometry: Investigation of Polyethylene Glycol-Conjugate Superoxide Dismutase, *J. Am. Soc. Mass Spectrom.*, **6**: 478–487.
38. Na, D.H., Youn, Y.S. and Lee, K.C. (2003). Optimization of the Pegylation Process of a Peptide by Monitoring with Matrix-assisted Laser Desorption/Ionization Time-Of-Flight Mass Spectrometry, *Rapid Commun. Mass Spectrom.*, **17**: 2241–2244.
39. Lauterwein, J., Brown, L.R. and Wüthrich, K. (1980). High-Resolution 1H-NMR Studies of Monomeric Melittin in Aqueous Solution, *Biochim. Biophys. Acta*, **622**: 219–230.
40. Digilio, G., Barbero, L., Bracco, C., Corpillo, D., Esposito, P., Piquet, G. et al. (2003). NMR Structure of Two Novel Polyethylene Glycol Conjugates of the Human Growth Hormone-Releasing Factor, Hgrf(1–29)-NH_2, *J. Am. Chem. Soc.*, **125**: 3458–3470.
41. Belcheva, N., Baldwin, S.P. and Saltzman, W.M. (1998). Synthesis and Characterization of Polymer-(Multi)-Peptide Conjugates for Control of Specific Cell Aggregation, *J. Biomater. Sci. Polym. End.*, **9**: 207–226.
42. Zhang, L., Furst, E.M. and Kiick, K.L. (2006). Manipulation of Hydrogel Assembly and Growth Factor Delivery via the Use of Peptide-Polysaccharide Interactions, *J. Control. Rel.*, **114**: 130–142.
43. Okada, A., Wakamatsu, K., Miyazawa, T. and Higashijima, T. (1994). Vesicle-Bound Conformation of Melittin: Transferred Nuclear Overhauser Enhancement Analysis in the Presence of Perdeuterated Phosphatidylcholine Vesicles, *Biochemistry*, **33**: 9438–9446.
44. Vig, S., Chitolie, A., Bevan, D., Haliday, A. and Dormandy, J. (2001). Thromboelastography: A Reliable Test? *Blood Coagul. Fibrinolysis*, **12**: 555–561.
45. Zhao, H., Rubio, B., Sapra, P., Wu, D., Reddy, P., Sai, P. et al. (2008). Novel Prodrugs of SN38 Using Multiarm Poly(Ethylene Glycol) Linkers, *Bioconjug. Chem.*, **19**: 849–859.
46. Yu, H., Feng, Z.-G., Zhang, A.-Y., Sun, L.-G. and Qian, L. (2006). Synthesis and Characterization of Three-Dimensional Crosslinked Networks Based on Self-Assembly of α-Cyclodextrins with Thiolated 4-Arm PEG Using a Three-Step Oxidation, *Soft Matter*, **2**: 343–349.
47. Wallace, D.G., Cruise, G.M., Rhee, W.M., Schroeder, J.A., Prior, J.J., Ju, J. et al. (2001). A Tissue Sealant Based on Reactive Multifunctional Polyethylene Glycol, *J. Biomed. Mater. Res.*, **58**: 545–555.

48. Seal, B.L. and Panitch, A. (2006). Physical Matrices Stabilized by Enzymatically Sensitive Covalent Crosslinks, *Acta Biomater.*, **2**: 241–251.
49. Xu, H., Kaar, J.L., Russell, A.J. and Wagner, W.R. (2006). Characterizing the Modification of Surface Proteins with Poly(Ethylene Glycol) to Interrupt Platelet Adhesion, *Biomaterials*, **27**: 3125–3135.
50. Na, D.H., Youn, Y.S. and Lee, K.C. (2003). Optimization of the Pegylation Process of a Peptide by Monitoring with Matrix-Assisted Laser Desorption/ Ionization Time-Of-Flight Mass Spectrometry, *Rapid Commun. Mass Spectrom.*, **17**: 2241–2244.
51. Larson, R.S., Menard, V., Jacobs, H. and Kim, S.W. (2001). Physicochemical Characterization of Poly(Ethylene Glycol)-Modified Anti-GAD Antibodies, *Bioconjug. Chem.*, **12**: 861–869.
52. Barker, T.H., Fuller, G.M., Klinger, M.M., Feldman, D.S. and Hagood, J.S. (2001). Modification of Fibrinogen with Poly(Ethylene Glycol) and its Effects on Fibrin Clot Characteristics, *J. Biomed. Mater. Res.*, **56**: 529–535.
53. Ramalingam, K., Bello, J. and Aimoto, S. (1993). Permethylation Alters the Conformational Transitions and the Complexing Ability of Melittin: A Model for Methylated Proteins, *Biopolymers*, **33**: 305–314.
54. Sumbatyan, N.V., Mandrugin, V.A., Deroussent, A., Bertrand, J.R., Majer, Z., Malvy, C. et al. (2004). The Solution Synthesis of Antisense Oligonucleotide–Peptide Conjugates Directly Linked via Phosphoramide Bond by Using a Fragment Coupling Approach, *Nucleos. Nucleot. Nucleic Acids*, **23**: 1911–1927.
55. Kinstler, O.B., Brems, D.N., Lauren, S.L., Paige, A.G., Hamburger, J.B. and Treuheit, M.J. (1996). Characterization and Stability of N-terminally PEGylated rhG-CSF, *Pharm. Res.*, **13**: 996–1002.
56. Maulet, Y., Mathey-Prevot, B., Kaiser, G., Rüegg, U.T. and Fulpius, B.W. (1980). Purification and Chemical Characterization of Melittin and Acetylated Derivatives, *Biochim. Biophys. Acta*, **625**: 274–280.
57. Morpurgo, M. and Veronese, F.M. (2004). Conjugates of Peptide and Proteins to Polyethylene Glycol, *Methods Mol. Biol.*, **283**: 45–70.
58. Goto, Y. and Hagihara, Y. (1992). Mechanism of the Conformational Transition of Melittin, *Biochemistry*, **31**: 732–738.
59. Kemple, M.D., Buckley, P., Yuan, P. and Prendergast, F.G. (1997). Main Chain and Side Chain Dynamics of Peptides in Liquid Solution from 13C NMR: Melittin as a Model Peptide, *Biochemistry*, **36**: 1678–1688.
60. Stigsnaes, P., Frokjaer, S., Bjerregaard, S., van de Weert, M., Kingshott, P. and Moeller, E.H. (2007). Characterisation and Physical Stability of PEGylated Glucagon, *Int. J. Pharm.*, **330**: 89–98.
61. Ius, A., Bacigalupo, M.A., Longhi, R. and Meroni, G. (2000). Selectively Conjugated Melittins for Liposome Time-Resolved Fluoroinnumoassay of Theophylline in Serum, *Fresenius J. Anal. Chem.*, **366**: 869–872.

62. Werkmeister, J.A., Hewish, D.R., Kirkpatrick, A. and Rivett, D.E. (2002). Sequence Requirements for the Activity of Membrane-active Peptides, *J. Pept Res.*, **60**: 232–238.
63. Blondelle, S.E. and Houghten, R.A. (1991). Hemolytic and Antimicrobial Activities of the Twenty-Four Individual Omission Analogues of Melittin, *Biochemistry*, **30**: 4671–4678.
64. Lin, S.C., Huang, T.F. and Ouyang, C. (1983). Characterization of the Purified Anticoagulant Principles from Apis Mellifera (Honey Bee) Venom, *J. Formos. Med. Assoc.*, **82**: 629–639.